AMERICAN SOCIETY of
GENE & CELL
THERAPY

Motor-Coordinative and Cognitive Dysfunction Caused by Mutant TDP-43 Could Be Reversed by Inhibiting Its Mitochondrial Localization

Wenzhang Wang,[1,3] Hiroyuki Arakawa,[2,3] Luwen Wang,[1,3] Ogoegbunam Okolo,[1] Sandra L. Siedlak,[1] Yinfei Jiang,[1] Ju Gao,[1] Fei Xie,[1] Robert B. Petersen,[1] and Xinglong Wang[1]

[1]Department of Pathology, Case Western Reserve University and University Hospitals Case Medical Center, Cleveland, OH 44106, USA; [2]Rodent Behavioral Core, School of Medicine, Case Western Reserve University, Cleveland, OH 44106, USA

Dominant missense mutations in TAR DNA-binding protein 43 (TDP-43) cause amyotrophic lateral sclerosis (ALS), and the cytoplasmic accumulation of TDP-43 represents a pathological hallmark in ALS and frontotemporal lobar degeneration (FTD). Behavioral investigation of the transgenic mouse model expressing the disease-causing human TDP-43 M337V mutant (TDP-43^{M337V} mice) is encumbered by premature death in homozygous transgenic mice and a reported lack of phenotype assessed by tail elevation and footprint in hemizygous transgenic mice. Here, using a battery of motor-coordinative and cognitive tests, we report robust motor-coordinative and cognitive deficits in hemizygous TDP-43^{M337V} mice by 8 months of age. After 12 months of age, cortical neurons are significantly affected by the mild expression of mutant TDP-43, characterized by cytoplasmic TDP-43 mislocalization, mitochondrial dysfunction, and neuronal loss. Compared with age-matched non-transgenic mice, TDP-43^{M337V} mice demonstrate a similar expression of total TDP-43 but higher levels of TDP-43 in mitochondria. Interestingly, a TDP-43 mitochondrial localization inhibitory peptide abolishes cytoplasmic TDP-43 accumulation, restores mitochondrial function, prevents neuronal loss, and alleviates motor-coordinative and cognitive deficits in adult hemizygous TDP-43^{M337V} mice. Thus, this study suggests hemizygous TDP-43^{M337V} mice as a useful animal model to study TDP-43 toxicity and further consolidates mitochondrial TDP-43 as a novel therapeutic target for TDP-43-linked neurodegenerative diseases.

INTRODUCTION

TAR DNA-binding protein 43 (TDP-43, also named ALS10) is a small, ubiquitously expressed RNA/DNA binding protein structurally resembling the family of RNA-binding protein heterogeneous nuclear ribonucleoproteins (hnRNPs).[1–3] Like hnRNPs, TDP-43 contains two tandem RNA recognition motifs, RRM1 and RRM2, that belong to the widely distributed eukaryotic RNA recognition motif family (RRM, also referred as RNA binding domain [RBD] or ribonucleoprotein domain [RNP]).[4] Although TDP-43 was initially identified as a transcriptional factor binding TAR DNA sequence motifs of human immunodeficiency virus type 1 and repressing gene transcrip-

tion,[5] subsequent studies have revealed that TDP-43 primarily binds mRNA and regulates post-transcriptional RNA processing, including RNA splicing, transportation, and translation.[1–3]

The breakthrough regarding TDP-43 research came from studies revealing that mutations in the TDP-43 gene cause both familial and sporadic amyotrophic lateral sclerosis (ALS, also called Lou Gehrig's disease), the most common of the five motor neuron diseases, characterized by progressive loss of motor neurons in the brain stem and spinal cord. TDP-43 is the major component of neuronal inclusions, the histopathological hallmark of both ALS and the most frequent subtypes of frontotemporal dementia (FTD), considered the second most common early-onset dementia, characterized by neuronal loss in the frontal and temporal cortex.[6,7] In fact, cytoplasmic TDP-43 accumulation also represents a secondary pathological feature of other major neurodegenerative diseases, including Alzheimer's disease,[8] Parkinson's disease,[9] and Huntington's disease.[10] Despite increasing evidence suggesting a critical role of TDP-43 in disease progression in these various major neurodegenerative diseases, the pathogenic mechanisms underlying TDP-43 are largely unknown.

Multiple transgenic animal models with TDP-43 overexpression or ablation have been generated to study the mechanisms of TDP-43-induced neuronal dysfunction in vivo.[11–20] However, either premature death before the presence of full behavior impairments or extremely aggressive disease progression in many of these animal models make the interpretation of behavioral and neuropathological measurements, especially cognitive assessment, difficult. The TDP-43^{M337V} transgenic (Tg) mouse (i.e., Prnp-TARDBP* M337V; The Jackson Laboratory, stock no. 017604) expresses the human TDP-43 M337V mutant under the direction of a mouse prion protein

CrossMark

promoter.[19] According to the initial study, phenotypes including body tremors, hindlimb clasping, and gait abnormality could only be observed in homozygous TDP-43^{M337V} Tg mice at 1 month of age (early stages of development) but are absent in hemizygous transgenic mice until 12 months of age,[19] and the premature sudden death renders homozygous mice unsuitable for testing cognitive tasks. So far, motor-coordinative and especially cognitive functions have not been extensively investigated in this transgenic mouse line. In this study, we performed a battery of motor-coordinative and cognitive tests in adult hemizygous TDP-43^{M337V} Tg mice. Based on our most recent study identifying mitochondria as critical direct mediators for TDP-43-induced neurotoxicity,[21] we further tested whether the inhibition of mutant TDP-43 mitochondrial localization could reverse motor-coordinative and cognitive deficits in aged hemizygous TDP-43^{M337V} Tg mice after disease onset.

RESULTS

Alterations in Motor Coordination, but Not Locomotive Activity, Muscle Strength, or Sensorimotor Function, in Adult Hemizygous TDP-43^{M337V} Mice

We first monitored hemizygous TDP-43^{M337V} mice by body weight and commonly used behavioral tests relevant to motor and coordination function: rotarod and beam walk tests. Hemizygous TDP-43^{M337V} mice were viable and phenotypically normal at birth and demonstrated no difference from wild-type (WT) littermates in feeding, body weight, survival, and hindlimb clasping until 16 months old (currently the oldest available mice; data not shown). However, at 8 months of age, they exhibited significant impairments in the performance of rotarod and beam walk tests, manifested by the decreased ability to stay on the rotarod and longer traverse latencies on beams ($F_{1,27}$ = 8.12, p < 0.01 for rotarod; $F_{1,27}$ = 11.86, p < 0.01 for 12-mm square beam; $F_{1,27}$ = 1.21, nonsignificant for 12-mm round beam; $F_{1,27}$ = 5.48, p < 0.05 for 9-mm square beam; Figures 1A and 1B). No difference in the rotarod and beam walk test was seen between male and female mice (Figures S1A and S1B). The impaired rotarod and beam-walking performance was not likely to be caused by muscle weakness because all mice performed similarly in the grip strength test for both fore- and hindlimbs ($F_{1,27}$ = 0.69 for forelimbs and 0.38 for hindlimbs, nonsignificant; Figure 1C).

To further investigate whether the locomotor activity was altered, we assessed the open field activity of transgenic mice. Compared with WT mice, 8- to 9-month-old hemizygous TDP-43^{M337V} mice showed a non-significant trend for greater traveling distance and faster moving speed in the open field test ($F_{1,27}$ = 3.55, p < 0.10 for distance; $F_{1,27}$ = 3.50, p < 0.10 for speed; Figure 1D). No difference in the time spent in the inner area was noted ($F_{1,27}$ = 0.05, nonsignificant; data not shown), indicating unchanged anxiety-related behavior. We also measured tactile sensory responses in hemizygous TDP-43^{M337V} mice by sticky paper test. The expression of TDP-43^{M337V} did not significantly affect the time for mice to make contact and remove adhesive tapes ($F_{1,27}$ = 0.02, nonsignificant; Figure 1E), suggesting that the paw sensorimotor function was not altered.

Cognitive Deficits in Adult TDP-43^{M337V} Tg Mice

Both the beam walk and especially the rotarod tests used to evaluate motor coordination may also be especially sensitive to brain dysfunction.[22–24] Therefore, the finding of impaired rotarod and beam-walking performance in hemizygous TDP-43^{M337V} mice, without deficits in locomotive activity, muscle strength, or sensorimotor function, might reflect behavioral alterations stemming from cognitive deficits in the brain. To test this hypothesis, we conducted a series of behavioral tests to investigate the cognitive performance in 8- to 9-month-old hemizygous TDP-43^{M337V} mice. The test battery consisted of a Y maze test for spatial working memory, a T maze test for short-term spatial memory, an object recognition test for short-term and long-term non-spatial memory, and a fear conditioning test for emotional memory. In the Y maze test, based on the natural tendency of mice to alternate arms when exploring a novel environment, all mice exhibited good ambulatory activity with similar exploration rates (data not shown). However, transgenic mice showed a significantly lower ratio of spontaneous alternations than WT mice ($F_{1,27}$ = 8.92, p < 0.01; Figure 2A), suggesting impaired spatial working memory. To further assess spatial memory deficits in hemizygous TDP-43^{M337V} mice, we performed a T maze test, also based on the innate preference of mice to explore unfamiliar environment relevant to visited arms. After the acclimation period, consistent with the Y maze test, transgenic mice performed significantly worse than age-matched WT mice ($F_{1,27}$ = 4.47, p < 0.05; Figure 2B).

In the object recognition test, utilizing the fact that animals will spend more time exploring a novel object compared with an object they are familiar with, no significant difference in the total amount of time spent to sniff and contact each object was evident during the first probe trial (T1, 50% chance level) for either group of mice ($F_{1,27}$ = 0.97, nonsignificant; Figure 2C). However, during the second dissimilar stimulus session (T2, short-term memory) and the third session 24 hr after T2 (T3, long-term memory), hemizygous TDP-43^{M337V} mice investigated unfamiliar objects significantly less than WT mice ($F_{1,27}$ = 22.73, p < 0.01 for T2; $F_{1,27}$ = 10.98, p < 0.01 for T3; Figure 2C), revealing impaired short-term and long-term non-spatial memory.

In the fear conditioning test, based on mice learning to associate a neutral tone conditional stimulus (CS) with a mild electrical foot unconditional stimulus (US) and show a freezing response, we did not detect any significant difference between WT and transgenic mice in the proportion of time spent freezing during habituation and first three US exposures in the training session ($F_{1,27}$ = 0.09 for the habituation session; $F_{1,27}$ = 0.003 for the first US; $F_{1,27}$ = 2.85 for the second US; $F_{1,27}$ = 1.83 for the third US; all nonsignificant; Figure 2D). Interestingly, in the fourth US exposure, hemizygous TDP-43^{M337V} mice showed significantly lower freezing times compared with WT mice ($F_{1,27}$ = 6.99, p < 0.05). The reduced fear response was indeed maintained in the test session 24 hr later to evaluate their learned aversion for an environment associated with the shock (context-dependent fear; $F_{1,27}$ = 4.94, p < 0.05). Cohorts of mice were also reintroduced into the contextually altered box (shape, lighting, and odor [vanilla essence]) for the cue-dependent fear conditioning test. Neither WT
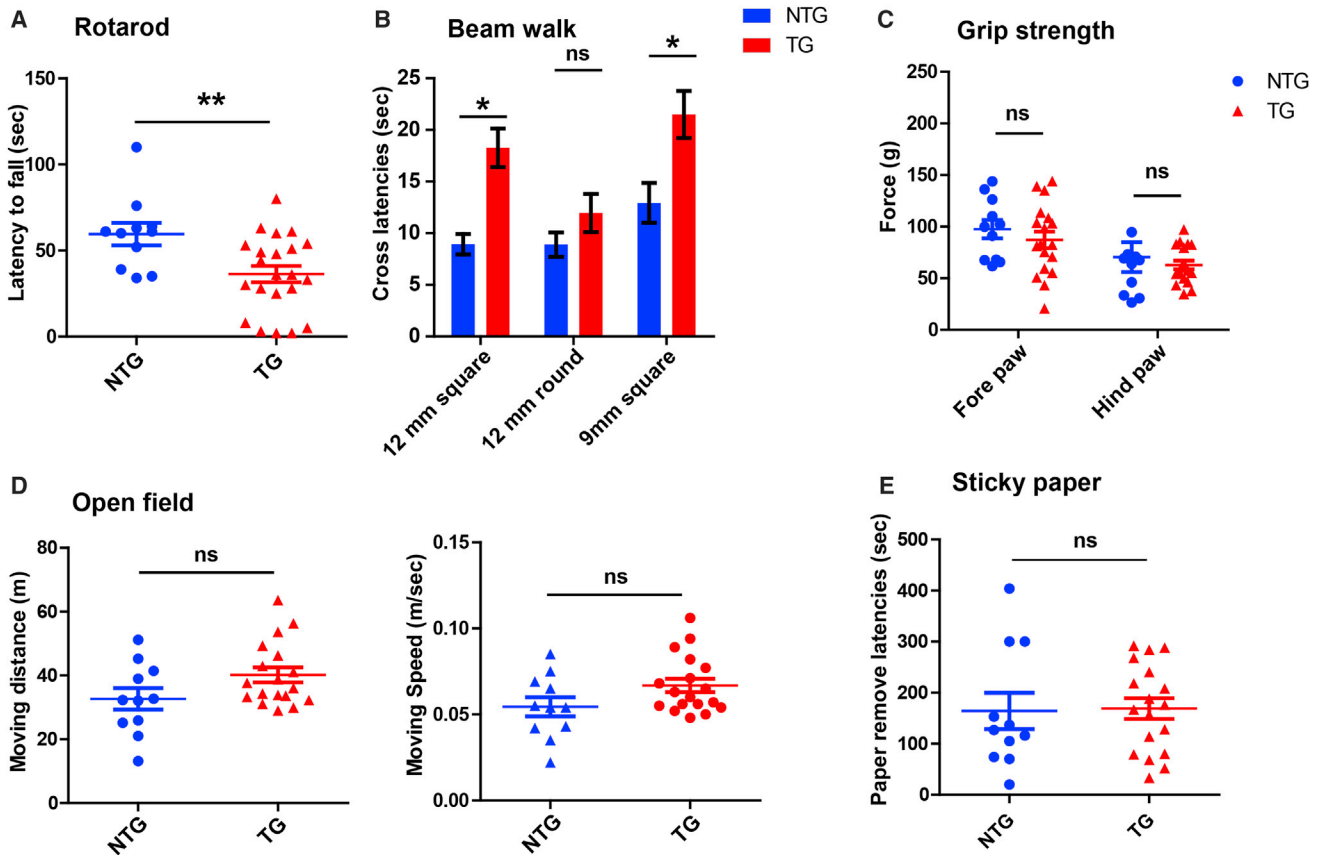
Figure 1. Sensorimotor Performances of Adult Hemizygous TDP-43^{M337V} Mice

(A) Motor coordination and balance in NTG and hemizygous TDP-43^{M337V} mice on the rotarod, manifested as the maximum time that mice could remain on the accelerating rotating rod. (B) Motor coordination and balance of mice in NTG and hemizygous TDP-43^{M337V} mice, assessed by the latency to traverse each beam. (C) Fore- and hindlimb strength of NTG and hemizygous TDP-43^{M337V} mice. (D) The distance traveled (meters) and velocity (meters per second) of non-transgenic age-matched littermate controls (NTG) and transgenic hemizygous TDP-43^{M337V} mice recorded continually for 10 min in the open field test. (E) Sensorimotor responses of NTG and hemizygous TDP-43^{M337V} mice, measured by the latency to remove a piece of adhesive tape from the hindpaw. All mice are at 8–9 months old. n = 11 for NTG (8 male/3 female) and 18 for TG (10 male/8 female). Data in the beam walk test were analyzed using two-way ANOVA followed by Bonferroni multiple comparisons, whereas data in other tests were analyzed using Student's t test. All data are presented as dots and means ± SEM; *p < 0.05, **p < 0.01; ns, non-significant.

nor transgenic mice could recognize the context before addition of the CS ($F_{1,27}$ = 2.44, nonsignificant). As expected, CS-elicited freezing responses were significantly lower in hemizygous TDP-43^{M337V} mice than in WT mice ($F_{1,27}$ = 7.59, p < 0.05). During extinction training with ten times CS exposure, both WT and transgenic mice displayed similar weak extinction (data not shown). In this study, no significance difference in the cognitive performance between male and female mice was noted (Figures S1C–S1F). In sum, our results show that, in addition to impaired motor and coordination function, adult hemizygous TDP-43^{M337V} mice also develop deficits in memory.

The Inhibition of TDP-43 Mitochondrial Localization by PM1 Alleviates Cytoplasmic TDP-43 Accumulation, Mitochondrial Dysfunction, and Neuronal Loss in the Brains of TDP-43^{M337V} Tg Mice

We previously characterized the specific amino acid motif that confers TDP43 mitochondrial localization.[21] The suppression of

TDP-43 mitochondrial localization by either the deletion of motif M1 (AQFPGACGL), essential for its mitochondrial localization, or treatment with the M1 motif-based inhibitory peptide PM1 could block WT or mutant TDP-43-induced mitochondrial dysfunction and neuronal death in vitro and in mice.[21] Here, 11- to 12-month-old WT and transgenic mice were continuously infused with PM1 or control peptide (cPM) for 6 weeks (1.5 mg/kg/day, subcutaneously implanted ALZET pumps). Consistent with our previous study,[21] murine TDP-43 (mTDP-43, recognized by a pan-TDP-43 antibody in WT mice) and human mutant TDP-43 (hTDP-43, recognized by an antibody specific to human TDP-43 in TDP-43^{M337V} mice) were present in highly purified mitochondria isolated from mouse brain tissues (Figure 3A). We confirmed that PM1 reached the central nervous system and substantially reduced the levels of endogenous mTDP-43 in mitochondria in the brains of WT mice (data not shown). Despite similar levels in total lysates, both total TDP-43 (mTDP-43 plus hTDP-43) and hTDP-43 displayed significantly
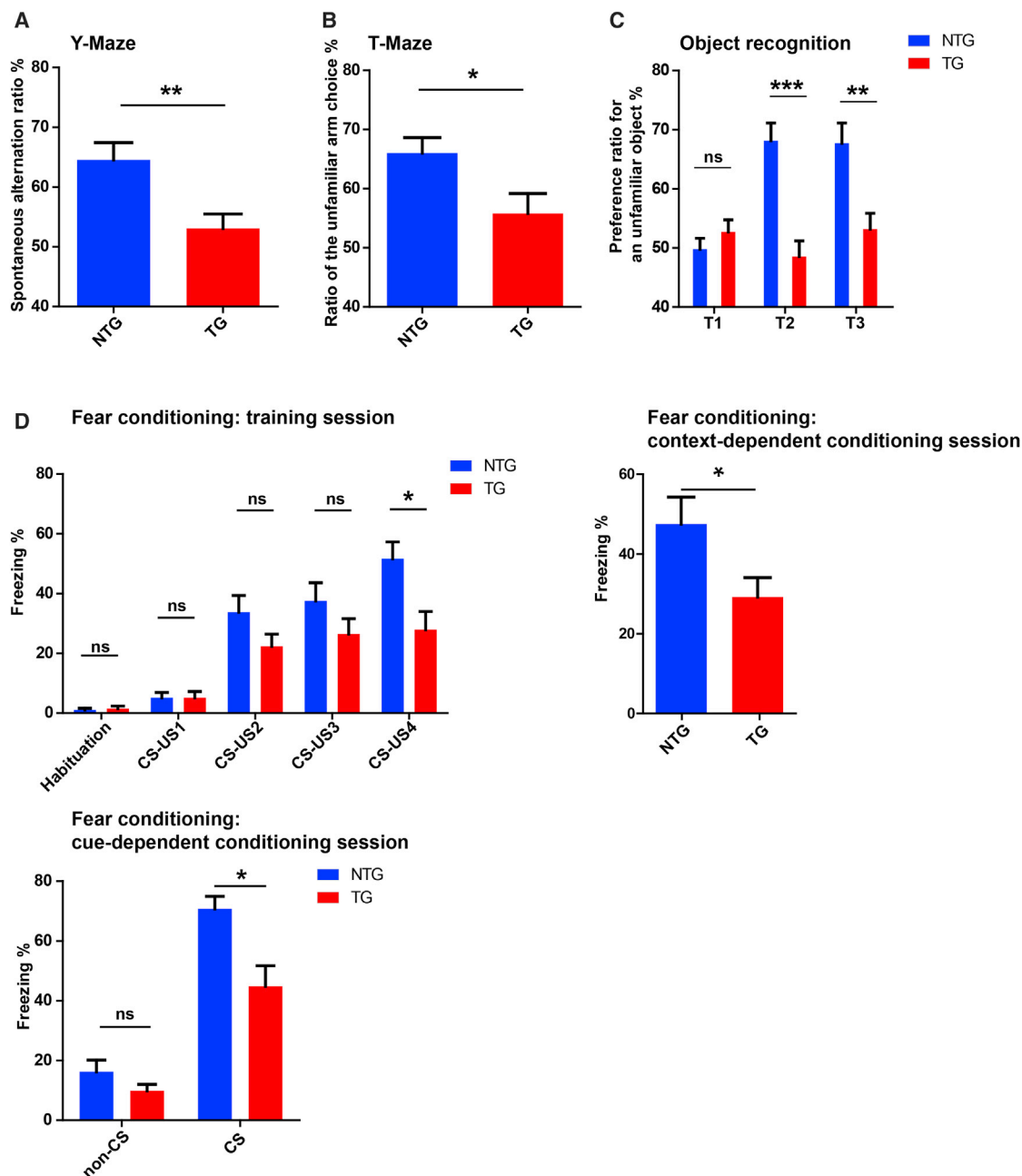
Figure 2. Cognitive Performances of Adult Hemizygous TDP-43^M337V Mice

(A and B) Spontaneous alternation of NTG and hemizygous TDP-43^M337V mice in the Y maze (A) and novelty preference in the T maze (B) test. (C) Preference ratio for an unfamiliar object of NTG and hemizygous TDP-43^M337V mice in the three different sessions of the object recognition test. T1, first 5-min trail session; T2, 1.5-hr-delayed 5-min dissimilar stimulus session; T3, 24-hr-delayed 5-min third session. (D) Freezing behavior of NTG and hemizygous TDP-43^M337V mice in the trail sessions (habituation without stimulus, repeated four times with inter-stimulus interval), contextual fear learning, and cue-dependent fear learning in the fear conditioning test. CS, white noise, 80 dB for 30 s; US, an electrical shock of 0.5 mA for 1 s. All mice were 8–9 months old. n = 11 for NTG (8 male/3 female) and 18 for TG (10 male/8 female). Data were analyzed using Student's t test or two-way ANOVA followed by Bonferroni multiple comparisons. All data are presented as means ± SEM; *$p < 0.05$, **$p < 0.01$, ***$p < 0.001$.

reduced expression in the mitochondrial fraction of hemizygous TDP-43^M337V mice after PM1 treatment (Figure 3A). Immunohisto-chemical analysis of TDP-43 using pan-TDP-43 antibodies found

TDP-43 accumulation in the cytoplasm of cortical neurons selec-tively in layers 2 and 3 in hemizygous TDP-43^M337V mice (Figures S2A and S2B). Further double labeling with a specific antibody to
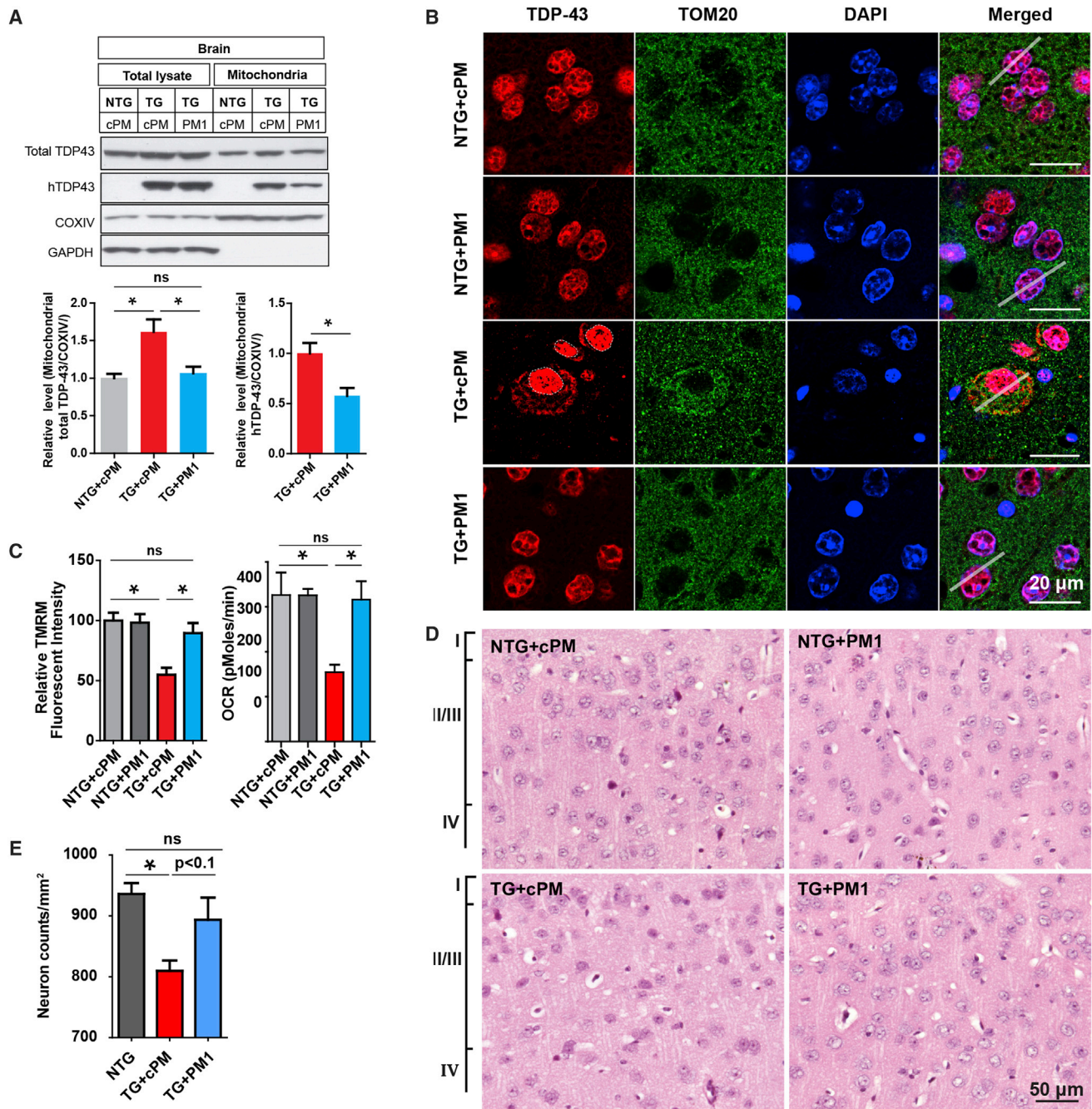
Figure 3. Inhibition of TDP-43 Mitochondrial Localization, Mitochondrial Dysfunction, and Neuronal Loss in the Brains of Hemizygous TDP-43^M337V Mice by PM1

11-month-old NTG and hemizygous TDP-43^M337V mice were treated with 1.5 mg/kg/day cPM (control peptide for PM1) or PM1 continuously for 6 weeks by subcutaneous infusion. NTG+cPM, NTG mice treated with cPM; NTG+PM1, NTG mice treated with PM1; TG+cPM, hemizygous TDP-43^M337V mice treated with cPM; TG+PM1, hemizygous TDP-43^M337V mice treated with PM1. (A) Representative immunoblot and quantification of exogenous human TDP-43 or total TDP-43 in total lysates and purified mitochondrial fraction of brains of NTG and TG mice treated with cPM or PM1 peptide. Equal amounts of 10 μg of proteins were loaded. Data are means ± SEM of triplicate experiments. (B) Representative confocal images of Tom20 (green) and TDP-43 (red) in cortical neurons co-stained using specific antibodies against Tom20 and TDP-43, respectively. Line scan analysis of the co-localization between Tom20 and TDP-43 as white solid lines by ImageJ RGB Profile Plot plugin is shown in Figure S2C. (C) Measurement of OCR/mΔψ in synaptic mitochondria in NTG and TG mice that were treated with the indicated peptide (n = 4 mice/group). Synaptosomes were isolated from mouse brains attached to Seahorse XF24 microplates or 24-well cell culture plates. The OCRs of synaptic mitochondria in synaptosomes were determined directly by

(legend continued on next page)

the mitochondrial protein TOM20 revealed that mislocalized TDP-43 highly co-localized with mitochondria (Figure 3B; Figures S2C and S2D). Interestingly, TDP-43 cytoplasmic accumulation in TDP-43[M337V] mice disappeared after PM1 peptide infusion, suggesting the prevention of TDP-43 mislocalization by PM1 (Figure 3B; Figures S2A and S2B).

TDP-43 in mitochondria impairs mitochondrial bioenergetics, and the inhibition of TDP-43 mitochondrial localization suppresses its toxicity on mitochondrial function.[21] Not surprisingly, the significant reduction of the mitochondrial membrane potential (m$\Delta\psi$) or oxygen consumption rate (OCR) noted in synaptic mitochondria isolated from brains of hemizygous TDP-43[M337V] mice was also greatly alleviated by PM1 (Figure 3C). PM1 alone did not change the basal levels of the m$\Delta\psi$ or OCR, which was consistent with our previous findings.[21] Intriguingly, 12-month-old, but not 8-month-old, hemizygous TDP-43[M337V] mice showed loss of cortical neurons most significantly in cortical layers 2 and 3 (Figures 3D and 3E; Figure S3; 8-month-old mice not shown), correlating with the TDP-43 mislocalization observed in these restricted cortical areas. After PM1 treatment, the neuronal density in cortical layers 2 and 3 in hemizygous TDP-43[M337V] mice was comparable with WT mice or WT mice treated with cPM, indicating the complete prevention of mutant TDP-43 M337V-induced neuronal loss by PM1. No apparent neuronal loss was seen in the hippocampus, cerebellum, or spinal cord (data not shown).

PM1 Reverses Motor Coordination and Cognitive Deficits in TDP-43[M337V] Tg Mice

Considering the protective effect of PM1 peptide treatment on mitochondria and neurons, we finally addressed whether the suppression of TDP-43 mitochondrial localization by PM1 was able to reverse behavior deficits in hemizygous TDP-43[M337V] mice after symptom onset. 11- to 12-month-old WT or transgenic mice were treated by PM1 or cPM via continuous subcutaneous infusion for 6 weeks. We confirmed that there was no significant difference in the rotarod and beam walk tests between cohorts of transgenic mice for PM1 and cPM infusion before treatment (p > 0.1 for rotarod, data not shown; $F_{1,16}$ = 1.51/0.18/0.01 for 12-mm square/12-mm round/9-mm square beam walking, nonsignificant; Figure S4). Compared with WT mice treated with cPM (non-transgenic [NTG]/cPM group), transgenic mice with cPM infusion (Tg/cPM group), but not transgenic mice with PM1 infusion (Tg/PM1 group), exhibited significantly impaired rotarod and beam-walking performance ($F_{2,21}$ = 11.93, p < 0.001 for rotarod; $F_{2,21}$ = 3.3, p < 0.1 for 12-mm square beam; $F_{2,21}$ = 8.8, p < 0.01 for 12-mm round beam; $F_{2,21}$ = 9.61, p < 0.01 for 12-mm square beam; Figures 4A and 4B), indicating improved motor coordination and balance after PM1 infusion. No difference in grip strength, loco-

motor activities, or tactile sense was noted among all three groups ($F_{2,21}$ = 1.803, nonsignificant for the open field test; $F_{2,21}$ = 0.53 and $F_{2,21}$ = 0.37, nonsignificant for fore-/hindlimb grip strength; $F_{2,21}$ = 1.368, nonsignificant for the sticky paper test; Figures 4C–4E). Consistently, in addition to deficits in motor-coordinative function, significantly impaired memory was also seen in Tg/cPM mice ($F_{2,21}$ = 3.92, p < 0.05 for the Y maze; $F_{2,21}$ = 4.97, p < 0.05 for the T maze; $F_{2,21}$ = 1.43/7.22/5.16, p > 0.1/< 0.01/< 0.05 for T1–T3 sessions, respectively, in the novel object recognition test; $F_{2,21}$ = 1.31/4.35/8.55/3.08/4.19, p > 0.1/< 0.05/< 0.01/< 0.1/< 0.05 for habituation and first through fourth US exposures during the training session, respectively, in the fear conditioning test; $F_{2,21}$ = 7.93, p < 0.01 for context-dependent learning; $F_{2,21}$ = 0.68, nonsignificant, for the no-cue period in cue-dependent learning; $F_{2,21}$ = 7.84, p < 0.01 for the cue period in cue-dependent learning; Figures 5A–5D). In contrast, Tg/PM1 showed greatly restored cognition to the levels of NTG/cPM mice, indicating that PM1 improved cognitive function in hemizygous TDP-43[M337V] mice. Extinction was not observed in the fear conditioning test in all groups, probably because the CS stimuli (white noise) kept inducing freezing in mice ($F_{8,84}$ = 1.065, p > 0.1; data not shown). Taken together, these results indicate that the inhibition of TDP-43 mitochondrial localization by PM1 is sufficient to reverse motor coordination dysfunction and cognitive deficits in hemizygous TDP-43[M337V] mice after symptom onset.

DISCUSSION

Here we used a mutant TDP-43 transgenic mouse model (TDP-43[M337V] mice) to test whether the inhibition of TDP-43 mitochondrial localization is sufficient to rescue mutant TDP-43-induced behavior deficits. We, for the first time, found that the readily available TDP-43[M337V] mice with hemizygous transgene expression demonstrated robust behavior deficits in adulthood. Consistent with our most recent study,[21] TDP-43[M337V] mice showed significantly increased levels of TDP-43 in mitochondria, accompanied by mitochondrial dysfunction and neuronal loss. Importantly, a specific inhibitor, PM1, which specifically inhibited TDP-43 mitochondrial localization without side effects on TDP-43 nuclear targets, reversed mitochondrial, neuronal, and behavior impairments in TDP-43[M337V] mice after disease onset. Thus, our findings suggest that mitochondrial TDP-43 could also be a promising therapeutic target for TDP-43-linked brain diseases.

In this study, we characterized behaviors in the previously generated transgenic mice expressing human TDP-43 bearing the M337V mutant. TDP-43[M337V] mice with hemizygous transgene expression demonstrated significant impairments of motor coordination and balance and a broad range of memory performances, including working spatial memory, short-term spatial memory, declarative

Seahorse, whereas m$\Delta\psi$ was measured by a fluorescence microplate reader after 20 nM tetramethylrhodamine methyl ester (TMRM) loading for 30 min. (D and E) Representative H&E-stained sections (D) and quantification (E) showing reduced neuronal density in mouse cortex layers 2 and 3 of TG mice with cPM (Tg mice without cPM treatment showed similar patterns; data not shown). In contrast, TG mice treated with PM1 showed comparable neuronal density and morphology, similar to NTG mice or NTG mice treated with cPM1 or PM1. All mice were 12–13 months old. n = 5 for NTG, 4 for TG+cPM, and 3 for TG+PM1. Data were analyzed using two-way ANOVA followed by Bonferroni multiple comparisons. *p < 0.05.
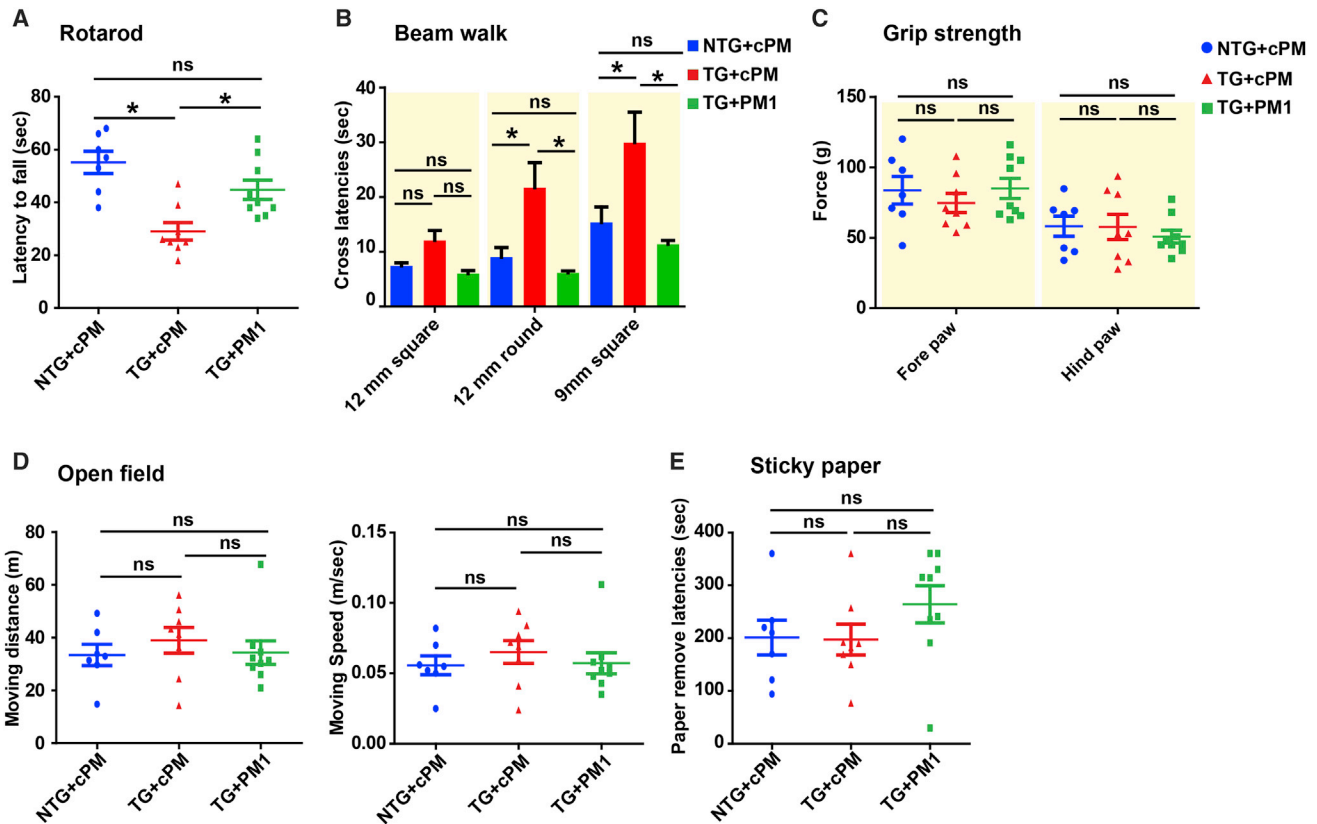
Figure 4. Improved Motor Coordination Performances of Adult Hemizygous TDP-43^{M337V} Mice by PM1

11-month-old NTG and hemizygous TDP-43^{M337V} mice were treated with 1.5 mg/kg/day cPM (control peptide for PM1) or PM1 continuously for 6 weeks by subcutaneous infusion. NTG+cPM, NTG mice treated with cPM; TG+cPM, hemizygous TDP-43^{M337V} mice treated with cPM; TG+PM1, hemizygous TDP-43^{M337V} mice treated with PM1. (A–E) Sensorimotor performances of NTG+cPM, TG+cPM, and TG+PM1 mice in the rotarod (A), beam walk (B), fore-/hindlimb strength (C), open field (D), and sticky paper test (E). All mice were 12–13 months old. n = 7 for NTG+cPM (4 male/3 female), 8 for TG+cPM (4 male/4 female), and 9 for TG+PM1 (5 male/4 female). Data were analyzed using ANOVA followed by Bonferroni multiple comparisons. All data are presented as dots and means ± SEM; *p < 0.05.

non-spatial memory, and associative fear learning. Surprisingly, locomotor activity, muscle strength, and tactile sensory function remained unchanged in hemizygous TDP-43^{M337V} mice until 16 months old (the oldest mice studied). Because significant neuronal loss was only seen in brain neurons but not in spinal cord motor neurons, it appeared that behavior deficits in hemizygous TDP-43^{M337V} mice, including poor rotarod or beam-walking performance, were likely caused by dysfunction or loss of brain neurons rather than spinal cord motor neurons. Although some studies showed the absence of dementia in patients bearing the M337V mutation,[7,25] one study from Kirby et al.[26] reported intellectual impairment in a patient from a family bearing the M337V mutant with very early disease onset at 2.5 years of age. In fact, some TDP-43 mutations have been identified in FTD patients without motor neuron disease.[27] Of note, mitochondrial dysfunction was not restricted to cortical neurons and could also be observed in spinal cord motor neurons in hemizygous TDP-43^{M337V} mice (data not shown), suggesting that cortical neurons and spinal cord motor neurons are both targets of the TDP-43 M337V mutant. In addition, although premature sudden

death prevented the assessment of cognitive function in previous studies using mutant TDP-43 transgenic animal models, cortical neuron degeneration has been consistently observed.[11,14,19,20,28] Therefore, our findings in hemizygous TDP-43^{M337V} mice do not necessarily contradict previous findings only reporting motor dysfunction in TDP-43 transgenic mice. Unlike other transgenic animal models showing increased expression of total TDP-43, the hemizygous TDP-43^{M337V} model does not demonstrate significantly changed expression of total TDP-43 in the brain and spinal cord,[29] indicating very low transgene expression. It is possible, therefore, that the level of TDP-43 M337V in hemizygous TDP-43^{M337V} mice is insufficient to reach the threshold necessary to cause spinal cord motor neuronal death, a feature required for the onset of ALS-like phenotypes such as muscle weakness and paralysis. Nevertheless, although our results indicate the likely association of brain neurons with behavior deficits in adult hemizygous TDP-43^{M337V} mice, the appearance of motor neuron loss or ALS-like behaviors in aged or extremely aged mice could not be ruled out, and future studies are needed to clarify these aspects.
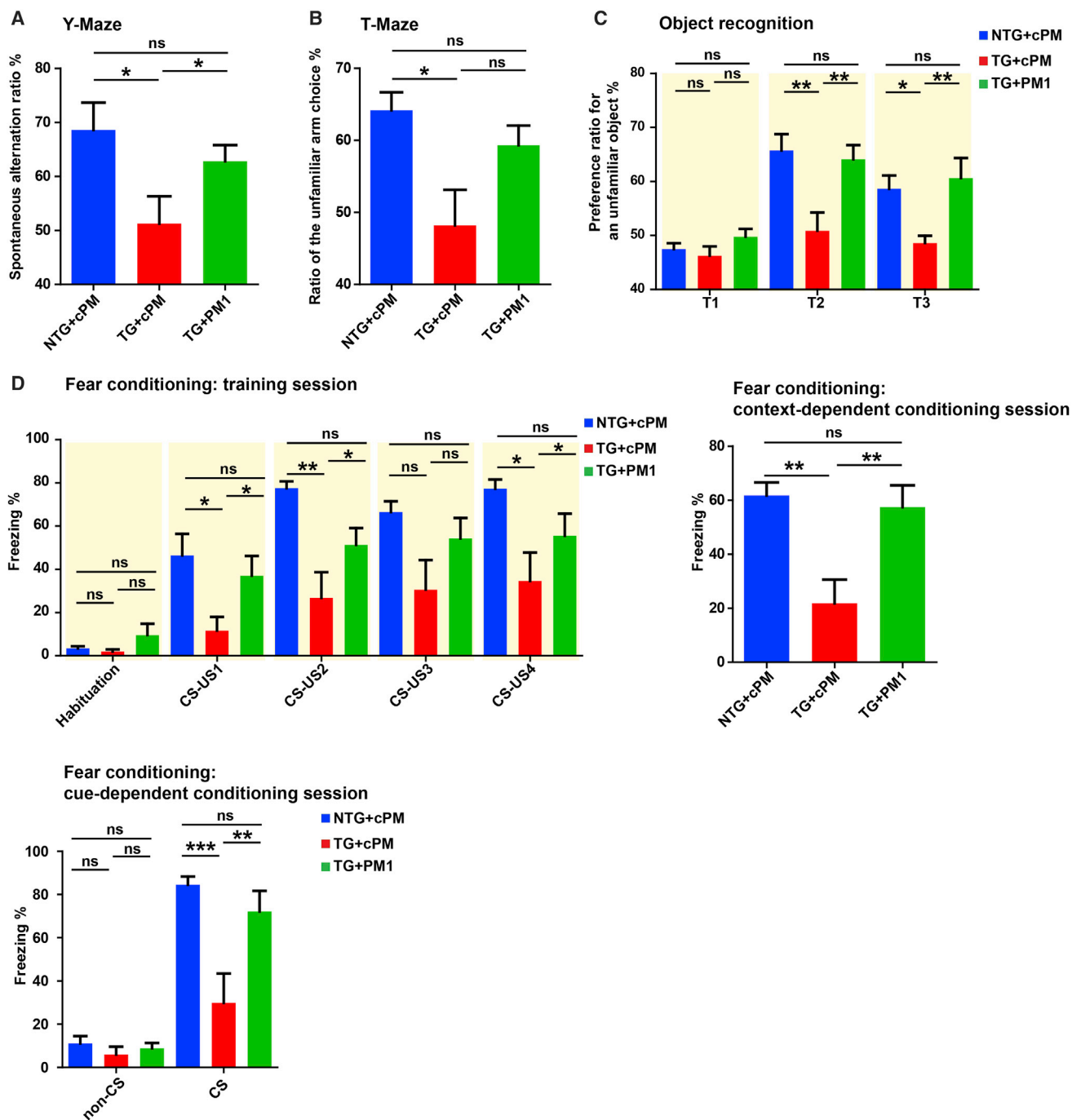
Figure 5. Improved Cognitive Performances of Adult Hemizygous TDP-43^{M337V} Mice by PM1

11-month-old NTG and hemizygous TDP-43^{M337V} mice were treated with 1.5 mg/kg/day cPM (control peptide for PM1) or PM1 continuously for 6 weeks by subcutaneous infusion. NTG+cPM, NTG mice treated with cPM; TG+cPM, hemizygous TDP-43^{M337V} mice treated with cPM; TG+PM1, hemizygous TDP-43^{M337V} mice treated with PM1. (A–D) Cognitive performances of NTG+cPM, TG+cPM, and TG+PM1 mice in the Y maze (A), T maze (B), object recognition test (C), and fear conditioning test (D). All mice were 12–13 months old. n = 7 for NTG+cPM (4 male/3 female), 8 for TG+cPM (4 male/4 female), and 9 for TG+PM1 (5 male/4 female). Data were analyzed using ANOVA followed by Bonferroni multiple comparisons. All data are presented as means ± SEM; *p < 0.05, **p < 0.01, ***p < 0.001.

TDP-43 mislocalization from the nucleus to the cytoplasm is a prominent pathological feature in various major neurodegenerative diseases. Not surprisingly, there has been a great deal of debate about whether loss of TDP-43 function via nuclear depletion or gain of neuronal toxicity by cytoplasmic TDP-43 accumulation causes neurodegeneration. Recent studies demonstrated that nuclear depletion was not required for TDP-43 neuronal toxicity[20,31] and that cytoplasmic TDP-43 was sufficient to cause neurodegeneration,[32] highlighting the critical role of cytoplasmic TDP-43 in disease progression. In fact, understanding the pathomechanisms of TDP-43, especially cytoplasmic TDP-43, is the major focus in the fields of ALS, FTD, and other neurodegenerative diseases linked to TDP-43. Interestingly, we have recently reported the accumulation of TDP-43 inside of mitochondria in patients with ALS or FTD and by ALS-associated mutations.[21] Similar to other TDP-43 mutations, compared with WT TDP-43, M337V also significantly increased TDP-43 import into mitochondria in vitro and in vivo (data not shown). Based on identified motifs essential for TDP-43 mitochondrial localization, we designed an inhibitory peptide, PM1, that could specifically suppress WT or mutant TDP-43 mitochondrial import without effect on the expression of nuclear, cytosolic, and total TDP-43.[21] We showed that PM1 could prevent motor dysfunction as well as spinal cord motor neuron death in hemizygous TDP-43[A315T] transgenic mice[21] (Prnp-TARDBP*A315T mice, also available from The Jackson Laboratory, stock no. 010700). Interestingly, TDP-43[A315T] mice also displayed significant loss of brain neurons, which could be abolished by PM1 treatment.[21] Unfortunately, premature death and gut problems make further assessments of brain-related cognitive function in this animal model difficult. Compared with TDP-43[A315T] mice, hemizygous TDP-43[M337V] mice demonstrated low transgene expression and the absence of early lethality, sudden death, or gait loss until at least 16 months of age, which could not only exclude potential side effects caused by transgene overexpression but also allow the full development of phenotypes after adulthood. In this study, using hemizygous TDP-43[M337V] mice as an animal model with robust behavior deficits, we showed that PM1 could also greatly alleviate mutant TDP-43-induced motor coordination and cognitive impairments. Thus, this study, together with our most recent report, strongly suggests that mitochondrial localization is a critical determinant of TDP-43 neurotoxicity and that the inhibition of mitochondrial TDP-43 could be a very promising therapeutic approach for TDP-43-linked brain or spinal cord diseases.

Cytoplasmic TDP-43 accumulation, the prominent feature of ALS and FTD, was recapitulated in cortical neurons of hemizygous TDP-43[M337V] mice. Interestingly, consistent with our previous study,[21] this TDP-43 proteinopathy could also be abolished by PM1 treatment, suggesting TDP-43 mitochondrial accumulation as a likely pathological event upstream of TDP-43 mislocalization. Cytoplasmic protein aggregation affects nucleocytoplasmic import and export.[33] Therefore, it might be interesting to test whether TDP-43 mitochondrial accumulation also interferes with nuclear transport factors to regulate nucleocytoplasmic transport. Previously reported mutant

TDP-43 animal models unanimously showed neuronal loss. However, none of these published studies could exclude the potential side effect caused by protein overexpression. This concern is indeed echoed by the fact that overexpression of WT TDP-43 itself is sufficient to cause neuronal dysfunction in mice.[16] Hemizygous TDP-43[M337V] mice exhibit neuronal death as well as phenotypes with unaltered total TDP-43 expression. Neuronal toxicity in this animal model should be specifically induced by the mutation but not likely as a result of human TDP-43 overexpression. It is still unclear how mutant TDP-43 induces age-dependent neurodegeneration. Although previous studies reported possibly different types of neuronal death caused by TDP-43, neuronal loss was not noticed in young hemizygous TDP-43[M337V] mice, and surviving neurons in adult hemizygous TDP-43[M337V] mice were cleaved caspase 3-negative (data not shown), suggesting that apoptosis is not likely to be involved. As a prominent common feature of ALS and other major neurodegenerative diseases,[34] mitochondrial dysfunction plays a critical role in almost all types of cell death, including apoptosis and necrosis.[35,36] We found that mitochondrial dysfunction could also be abolished by PM1 treatment. Thus, mitochondrial dysfunction observed in TDP-43[M337V] mice is likely the consequence of increased mitochondrial TDP-43. Nevertheless, although beyond the scope of the present study, hemizygous TDP-43[M337V] mice showing robust neurodegeneration and cognitive deficits could be very useful to explore the molecular mechanisms underlying mutant TDP-43-induced mitochondrial dysfunction and neuronal loss in the context of aging.

In summary, we show robust aged-dependent neurodegeneration and impairments of motor coordination and balance and cognition in adult hemizygous TDP-43[M337V] mice. This previously developed animal model with unchanged expression of total TDP-43 and readily available from The Jackson Laboratory might be a very useful model to study neurodegeneration. Importantly, this study, together with our previous findings, consistently demonstrates that the inhibition of TDP-43 mitochondrial localization by PM1 is sufficient to reverse behavior deficits after symptom onset. Thus, mutant TDP-43 probably exerts its toxicity via increased localization in mitochondria. The development of PM1-like inhibitors targeting TDP-43 mitochondrial localization may be beneficial in the treatment of TDP-43-linked neurodegenerative disease.

MATERIALS AND METHODS
Animals and Treatments
Mouse surgery and procedures were performed according to NIH guidelines and were approved by the Institutional Animal Care and Use Committee (IACUC) at Case Western Reserve University. C57BL/6 non-transgenic wild-type C57BL/6 mice (NTG mice) and C57BL/6-Tg(Prnp-TARDBP*M337V)4Ptrc/J (hTDP-43[M337V] transgenic mice, stock no. 017604) were purchased from the The Jackson Laboratory and maintained at Case Western Reserve University. All mice were weaned on post-natal day 30 and genotyped by PCR analysis of DNA extracted from a punched ear. Detailed mouse age and gender information for each experiment is presented in specific figure

legends. For peptide infusion, mini osmotic pumps (Alzet model 2006, flow rate of 0.15 μL/hr) were filled with 200 μL PBS containing cPM or PM1 peptides (0.5 mg/kg/day) followed by pump incubation in PBS at 37°C overnight according to the manufacturer's instructions. When mice were fully anesthetized with avertin, mini osmotic pumps were implanted subcutaneously at the back of the mouse. Six weeks after treatment, mice were transcardially perfused with ice-cold PBS, and brain and spinal cord tissues were collected.

Behavioral Tests

A series of behavioral tests to investigate the sensorimotor and cognitive performances were conducted in mice treated with or without peptide infusion. The results from two independent but age-matched cohort groups were combined. The test battery consisted of a motor task (open field test), body coordination task (rotarod and beam walk test), muscle strength task (grip strength test), tactile sense task (sticky paper test), and memory task (Y maze for working memory, T maze for short-term spatial memory, object recognition for short-term and long-term non-spatial memory, and fear conditioning for emotional memory). Individual mice were tested for these behavioral tasks on each test day in the following order: day 1 for the rotarod and grip strength test, day 2 for the open field test and beam walk test, day 3 for the Y maze, days 4–5 for the sticky paper test and object recognition test, day 6 for the T maze, and days 7–8 for the fear conditioning test. All tests were performed at the Case Behavior Core, with the investigator blinded to both mouse genotype and treatment group.

Rotarod Test

Rota-Rods (Panlab/Harvard Apparatus) were used to measure motor coordination and balance. Each mouse first received three trials per day for 3 days. During the training period, each mouse was placed on the rotarod, where cylinder speed was gradually increased from 4 rpm to 12 rpm for each trial. On the testing day, the rotarod was set to accelerating mode (4–40 rpm over 5 min), and maximal latency to fall off was collected for statistical analysis.

Grip Strength Test

The muscular strength of a mouse was measured by a grip strength test meter (Bioseb). For the forelimb test, the two forepaws of a mouse were placed on a bar, and mouse's tail was pulled back. For the hindlimb test, the two forepaws were placed on a grid that was held by the examiner's left hand, and the two hindpaws of the mouse were placed on a bar that was connected to the machine. The single best recorded value was used for statistical analysis.

Open Field Test

The open field test consisted of a 50-cm-long square plastic apparatus, closed with 50-cm-high walls, and activity was recorded using ANY-maze video tracking software (Stoelting). The field was digitally divided into an inner area (30 × 30 cm) and periphery (10-cm-wide gallery) using ANY-maze software. Data were collected continually for 10 min, and the distance traveled (meters), velocity (meters per second), the time spent immobile (more than 2 s of non-locomo-

tion), and the time spent in the inner area were all recorded and scored automatically.

Beam Walk Test

The motor coordination and balance of mice were assessed by measuring the ability of the mice to traverse a graded series of narrow beams to reach an enclosed safety platform. The beams consisted of long strips of wood (50 cm) with a 16-mm round diameter or a 16- or 9-mm square cross-section. During training, the mice were placed at the start of the 16-mm round beam and trained to traverse the beam to the enclosed box. After the mice were trained (traversed the 16-mm round beam in less than 20 s), they received two consecutive trials on each of the beams, in each case progressing from the 16-mm round beam or 16-mm square beam to the 9-mm square beam. Mice were allowed up to 60 s to traverse each beam. The latency to traverse each beam and the number of times the fore- and hindfeet slipped off each beam were recorded for each trial.

Y Maze Test

To investigate their short-term special memory, mice were placed in a Plexiglas Y maze (with arms 60 cm in length) and allowed to explore the maze freely for 8 min while one of the arms was blocked. The blocked arm was switched between animals to avoid any arm preference bias (counterbalanced). Following an 8-min exploration, mice were returned to their home cage for 2 hr and then put back in the Y maze for 5 min, this time with all three arms open. When put in the Y maze, the mice were recorded using the ANY-maze tracking system, and the time and frequency in the previously blocked arm and total number of arm entries were counted.

T Maze Test

To investigate their short-term special memory, mice were placed in a Plexiglas T maze (with arms 60 cm in length) and allowed to explore the maze freely for 10 min while one of the arms was blocked. The blocked arm was switched between animals to avoid any arm preference bias (counterbalanced). Following a-10 min exploration, mice were returned to their home cage for 2 hr and then put back in the T maze, this time with all three arms open. When put in the T-maze, the mice were recorded using the ANY-maze tracking system (Stoelting), and the time and frequency in the previously blocked arm and total number of arm entries were counted by using video scoring software.

Object Recognition Test

This task of recognition memory utilizes the fact that animals will spend more time exploring a novel object compared with an object they are familiar with. The test apparatus was a regular housing cage with bedding material. Each mouse was placed in a regular housing cage for 3 min. Then, two identical objects were placed at the corner of the housing cage (T1). The mice were allowed to investigate these objects for 5 min. This session was followed by a 1.5-hr delay during which the animals were returned to their home cages with their cagemates. After the delay, the animals performed a 5-min dissimilar stimulus session (T2, short-term memory). In this session, an

object that was presented in T1 and another object that was unfamiliar were placed in the test cages. Then, mice were returned to their home cages, and, 24 hr later, the third session was performed (T3, long-term memory). In this 5-min session, an object that was presented in T1 and T2 and another object that was unfamiliar were placed in the test cages. The objects were made of hard plastic and/or metal with apparently different shapes. The total amount of time spent to sniff and contact each object was recorded and scored using fully automated ANY-maze video tracking software. The total distance travel during 5 min and the duration of stay at the far side of the cage (immobile) were also measured.

Fear Conditioning Test

All animals were placed in a conditioning box (Med Associates) and trained to associate a tone (white noise, 80 decibels [dB] for 30 s, CS) with electrical shock (0.5 mA for 1 s, US). This procedure was repeated four times with 120-s accumulation and a 60-s inter-stimulus-interval. Tone and shock were co-terminated. At the end of the trial, the animals were taken out and placed back in the box 24 hr later to evaluate their learned aversion for an environment associated with the shock (context-dependent fear). To this end, all animals were placed in the same box in which they were trained for the duration of 6 min, and freezing behavior in the absence of tone or aversive stimulus were measured. The animals were then removed, and the context was changed so that the animals could no longer recognize the chamber in which they had been trained. Two hours after the animals were tested for contextual fear conditioning, they were reintroduced into the now contextually altered box (shape, lighting, and odor [vanilla essence]), and freezing behavior was measured during the first 2 min to verify that the animals did not recognize the context. After 2 min (no-cue period), the tone (30 s, 5 kHz, 80 dB) was delivered 10 times without US exposure in 60-s intertone interval (ISI), and freezing behavior was measured to determine cue-dependent fear conditioning.

Mitochondrial Isolation

Tissue was homogenized in IB-1 solution (225 mM mannitol, 75 mM sucrose, 0.1 mM EGTA, and 20 mM 4-(2-hydroxyethyl)-1-piperazineethanesulfonic acid [HEPES] [pH 7.4]). Then the homogenate was centrifuged at $600 \times g$ for 5 min to remove nuclear contaminants and unbroken cells. The supernatant was again centrifuged at $600 \times g$ for 5 min, followed by centrifugation at $7,000 \times g$ for 10 min. The supernatant was collected as the cytosolic fraction. The pellet was washed in IB-2 solution (225 mM mannitol, 75 mM sucrose, and 20 mM HEPES [pH 7.4]), centrifuged at $7,000 \times g$ for 10 min, resuspended in IB-2 solution, centrifuged at $10,000 \times g$ for 10 min, and finally resuspended in mitochondria resuspending buffer (MRB) (250 mM mannitol, 5 mM HEPES, and 0.5 mM EGTA [pH 7.4]). The resuspended fraction was overlaid on top of 8 mL Percoll medium (225 mM mannitol, 25 mM HEPES [pH 7.4], 1 mM EGTA, and 30% Percoll [v/v]), followed by centrifugation at $95,000 \times g$ in a SW40 rotor for 30 min at 4°C. The purified mitochondrial fraction was collected and resuspended in a 10-fold volume of MRB and centrifuged for 10 min at $6,300 \times g$ to collect the pellet as mitochondrial fraction.

Synaptosome Isolation and Mitochondrial Respiration Assay

Synaptosomes were isolated from mouse cortices as reported previously.[37,38] Briefly, cortex tissue was rapidly removed and homogenized in ice-cold sucrose medium (320 mM sucrose, 1 mM EDTA, 0.25 mM DTT (pH 7.4)). The homogenate was then centrifuged at $1,000 \times g$ for 10 min at 4°C. The supernatant was carefully layered on top of a discontinuous Percoll gradient (3-mL layers of 3%, 10%, and 23% Percoll in sucrose medium) in a centrifuge tube and centrifuged at $32,500 \times g$ for 10 min at 4°C. Synaptosomes were collected as the band between 10% and 23% Percoll. The collected solution was diluted into ionic medium (20 mM HEPES, 10 mM D-glucose, 1.2 mM Na_2HPO_4, 1 mM $MgCl_2$, 5 mM $NaHCO_3$, 5 mM KCl, and 140 mM NaCl [pH. 7.4]). After centrifugation at $15,000 \times g$ for 15 min at 4°C to remove Percoll, pellets were resuspended in ionic medium. The cell culture plates were coated with polyethyleneimine (1:15,000 dilution from a 50% solution, Sigma-Aldrich) overnight and washed with distilled water. The synaptosomes were attached to plates by centrifugation at $3,000 \times g$ at 4°C for 30 min and placed on ice for further measurement. The mitochondrial respiration assay protocol consisted of repeated cycles of 3-min mixing, 2-min waiting, and 3-min measurement periods. The basal OCR was measured three times by Seahorse XF-24 (Seahorse Bioscience). Protein concentrations for each well were measured to confirm the similar amount of synaptosomes.

Immunoblot, Immunocytochemistry, and Immunofluorescence Analysis

Tissues or the cellular fraction were homogenized or lysed in radio-immunoprecipitation assay (RIPA) buffer (Abcam) with $1\times$ protease inhibitor cocktail (Cell Signaling Technology). Proteins were separated by 10% SDS-PAGE and transferred to a polyvinylidene fluoride (PVDF) membrane. Following incubation with primary antibody overnight in a cold room and secondary antibodies at room temperature (RT) for 1 hr, immunoreactivity was detected by enhanced chemiluminescence (ECL) (Millipore Immobilon). The primary antibodies used included the following: rabbit TDP-43 antibody (Proteintech), mouse human TDP-43 antibody (Abnova), COX VI (Abcam), and GAPDH/Calnexin (Cell Signaling). Immunocytochemistry was performed by the peroxidase anti-peroxidase protocol.[39] For immunofluorescent staining, deparaffinized and re-hydrated tissue sections without H_2O_2 treatment were washed briefly three times with distilled H_2O and placed in $1\times$ antigen decloaker (Biocare). The sections were then subjected to antigen retrieval under pressure using Biocare's decloaking chamber by heating to125°C for 10 s and cooling to 90°C for 30 s, followed by heating to 22 psi at 128°C and cooling to 0 psi at 94°C. After the temperature decreased to 30°C, the sections were gradually rinsed with distilled H_2O five times. The sections were then blocked with 10% normal goat serum (NGS) for 30 min at RT and incubated with primary antibodies in PBS containing 1% NGS overnight at 4°C. After three washes with PBS, the sections were incubated in 10% NGS for 10 min and then with Alexa Fluor-conjugated secondary antibody (Life Technologies, 1:300) for 2 hr at RT in the dark. Finally, the sections were rinsed three times with PBS, stained with DAPI, washed again with PBS three times, and mounted with Fluoromount-G mounting medium (Southern Biotech).

Statistical Analysis

Statistical analysis was performed by ANOVA with Bonferroni correction or Student's t test (for two sets of data only). $p < 0.05$ was considered to be statistically significant.

SUPPLEMENTAL INFORMATION

Supplemental Information includes four figures and can be found with this article online at http://dx.doi.org/10.1016/j.ymthe.2016.10.013.

AUTHOR CONTRIBUTIONS

X.W. designed the experiments, prepared figures, and wrote the paper. H.A., W.W., and L.W. performed behavioral tests. W.W., L.W., O.O., S.L.S., Y.J., J.G., F.X., and X.W. carried out experiments related to the biochemical analysis of mice. H.A. and R.B.P. helped with data analysis and provided feedback on the manuscript.

CONFLICTS OF INTEREST

X.W. has a pending patent application related to PM1.

ACKNOWLEDGMENTS

REFERENCES

1. Buratti, E., and Baralle, F.E. (2008). Multiple roles of TDP-43 in gene expression, splicing regulation, and human disease. Front. Biosci. 13, 867–878.

2. Buratti, E., and Baralle, F.E. (2012). TDP-43: gumming up neurons through protein-protein and protein-RNA interactions. Trends Biochem. Sci. 37, 237–247.

3. Lee, E.B., Lee, V.M., and Trojanowski, J.Q. (2011). Gains or losses: molecular mechanisms of TDP43-mediated neurodegeneration. Nat. Rev. Neurosci. 13, 38–50.

4. Cléry, A., Blatter, M., and Allain, F.H. (2008). RNA recognition motifs: boring? Not quite. Curr. Opin. Struct. Biol. 18, 290–298.

5. Ou, S.H., Wu, F., Harrich, D., García-Martínez, L.F., and Gaynor, R.B. (1995). Cloning and characterization of a novel cellular protein, TDP-43, that binds to human immunodeficiency virus type 1 TAR DNA sequence motifs. J. Virol. 69, 3584–3596.

6. Kabashi, E., Valdmanis, P.N., Dion, P., Spiegelman, D., McConkey, B.J., Vande Velde, C., Bouchard, J.P., Lacomblez, L., Pochigaeva, K., Salachas, F., et al. (2008). TARDBP mutations in individuals with sporadic and familial amyotrophic lateral sclerosis. Nat. Genet. 40, 572–574.

7. Sreedharan, J., Blair, I.P., Tripathi, V.B., Hu, X., Vance, C., Rogelj, B., Ackerley, S., Durnall, J.C., Williams, K.L., Buratti, E., et al. (2008). TDP-43 mutations in familial and sporadic amyotrophic lateral sclerosis. Science 319, 1668–1672.

8. Amador-Ortiz, C., Lin, W.L., Ahmed, Z., Personett, D., Davies, P., Duara, R., Graff-Radford, N.R., Hutton, M.L., and Dickson, D.W. (2007). TDP-43 immunoreactivity in hippocampal sclerosis and Alzheimer's disease. Ann. Neurol. 61, 435–445.

9. Chanson, J.B., Echaniz-Laguna, A., Vogel, T., Mohr, M., Benoilid, A., Kaltenbach, G., and Kiesmann, M. (2010). TDP43-positive intraneuronal inclusions in a patient with motor neuron disease and Parkinson's disease. Neurodegener. Dis. 7, 260–264.

10. Davidson, Y., Amin, H., Kelley, T., Shi, J., Tian, J., Kumaran, R., Lashley, T., Lees, A.J., DuPlessis, D., Neary, D., et al. (2009). TDP-43 in ubiquitinated inclusions in the inferior olives in frontotemporal lobar degeneration and in other neurodegenerative diseases: a degenerative process distinct from normal ageing. Acta Neuropathol. 118, 359–369.

11. Wegorzewska, I., Bell, S., Cairns, N.J., Miller, T.M., and Baloh, R.H. (2009). TDP-43 mutant transgenic mice develop features of ALS and frontotemporal lobar degeneration. Proc. Natl. Acad. Sci. USA 106, 18809–18814.

12. Shan, X., Chiang, P.M., Price, D.L., and Wong, P.C. (2010). Altered distributions of Gemini of coiled bodies and mitochondria in motor neurons of TDP-43 transgenic mice. Proc. Natl. Acad. Sci. USA 107, 16325–16330.

13. Stallings, N.R., Puttaparthi, K., Luther, C.M., Burns, D.K., and Elliott, J.L. (2010). Progressive motor weakness in transgenic mice expressing human TDP-43. Neurobiol. Dis. 40, 404–414.

14. Tsai, K.J., Yang, C.H., Fang, Y.H., Cho, K.H., Chien, W.L., Wang, W.T., Wu, T.W., Lin, C.P., Fu, W.M., and Shen, C.K. (2010). Elevated expression of TDP-43 in the forebrain of mice is sufficient to cause neurological and pathological phenotypes mimicking FTLD-U. J. Exp. Med. 207, 1661–1673.

15. Wils, H., Kleinberger, G., Janssens, J., Pereson, S., Joris, G., Cuijt, I., Smits, V., Ceuterick-de Groote, C., Van Broeckhoven, C., and Kumar-Singh, S. (2010). TDP-43 transgenic mice develop spastic paralysis and neuronal inclusions characteristic of ALS and frontotemporal lobar degeneration. Proc. Natl. Acad. Sci. USA 107, 3858–3863.

16. Xu, Y.F., Gendron, T.F., Zhang, Y.J., Lin, W.L., D'Alton, S., Sheng, H., Casey, M.C., Tong, J., Knight, J., Yu, X., et al. (2010). Wild-type human TDP-43 expression causes TDP-43 phosphorylation, mitochondrial aggregation, motor deficits, and early mortality in transgenic mice. J. Neurosci. 30, 10851–10859.

17. Igaz, L.M., Kwong, L.K., Lee, E.B., Chen-Plotkin, A., Swanson, E., Unger, T., Malunda, J., Xu, Y., Winton, M.J., Trojanowski, J.Q., and Lee, V.M. (2011). Dysregulation of the ALS-associated gene TDP-43 leads to neuronal death and degeneration in mice. J. Clin. Invest. 121, 726–738.

18. Swarup, V., Phaneuf, D., Bareil, C., Robertson, J., Rouleau, G.A., Kriz, J., and Julien, J.P. (2011). Pathological hallmarks of amyotrophic lateral sclerosis/frontotemporal lobar degeneration in transgenic mice produced with TDP-43 genomic fragments. Brain 134, 2610–2626.

19. Xu, Y.F., Zhang, Y.J., Lin, W.L., Cao, X., Stetler, C., Dickson, D.W., Lewis, J., and Petrucelli, L. (2011). Expression of mutant TDP-43 induces neuronal dysfunction in transgenic mice. Mol. Neurodegener. 6, 73.

20. Arnold, E.S., Ling, S.C., Huelga, S.C., Lagier-Tourenne, C., Polymenidou, M., Ditsworth, D., Kordasiewicz, H.B., McAlonis-Downes, M., Platoshyn, O., Parone, P.A., et al. (2013). ALS-linked TDP-43 mutations produce aberrant RNA splicing and adult-onset motor neuron disease without aggregation or loss of nuclear TDP-43. Proc. Natl. Acad. Sci. USA 110, E736–E745.

21. Wang, W., Wang, L., Lu, J., Siedlak, S.L., Fujioka, H., Liang, J., Jiang, S., Ma, X., Jiang, Z., da Rocha, E.L., et al. (2016). The inhibition of TDP-43 mitochondrial localization blocks its neuronal toxicity. Nat. Med. 22, 869–878.

22. Carter, R.J., Morton, J., and Dunnett, S.B. (2001). Motor coordination and balance in rodents. Curr. Protoc. Neurosci. Chapter 8. Unit 8.12.

23. Brooks, S.P., and Dunnett, S.B. (2009). Tests to assess motor phenotype in mice: a user's guide. Nat. Rev. Neurosci. 10, 519–529.

24. Shiotsuki, H., Yoshimi, K., Shimo, Y., Funayama, M., Takamatsu, Y., Ikeda, K., Takahashi, R., Kitazawa, S., and Hattori, N. (2010). A rotarod test for evaluation of motor skill learning. J. Neurosci. Methods 189, 180–185.

25. Rutherford, N.J., Zhang, Y.J., Baker, M., Gass, J.M., Finch, N.A., Xu, Y.F., Stewart, H., Kelley, B.J., Kuntz, K., Crook, R.J., et al. (2008). Novel mutations in TARDBP (TDP-43) in patients with familial amyotrophic lateral sclerosis. PLoS Genet. 4, e1000193.

26. Kirby, J., Goodall, E.F., Smith, W., Highley, J.R., Masanzu, R., Hartley, J.A., Hibberd, R., Hollinger, H.C., Wharton, S.B., Morrison, K.E., et al. (2010). Broad clinical phenotypes associated with TAR-DNA binding protein (TARDBP) mutations in amyotrophic lateral sclerosis. Neurogenetics 11, 217–225.

27. Borroni, B., Bonvicini, C., Alberici, A., Buratti, E., Agosti, C., Archetti, S., Papetti, A., Stuani, C., Di Luca, M., Gennarelli, M., and Padovani, A. (2009). Mutation within TARDBP leads to frontotemporal dementia without motor neuron disease. Hum. Mutat. 30, E974–E983.

28. Zhou, H., Huang, C., Chen, H., Wang, D., Landel, C.P., Xia, P.Y., Bowser, R., Liu, Y.J., and Xia, X.G. (2010). Transgenic rat model of neurodegeneration caused by mutation in the TDP gene. PLoS Genet. 6, e1000887.

29. Zhang, F., Wang, W., Siedlak, S.L., Liu, Y., Liu, J., Jiang, K., Perry, G., Zhu, X., and Wang, X. (2015). Miro1 deficiency in amyotrophic lateral sclerosis. Front. Aging Neurosci. 7, 100.

31. Austin, J.A., Wright, G.S., Watanabe, S., Grossmann, J.G., Antonyuk, S.V., Yamanaka, K., and Hasnain, S.S. (2014). Disease causing mutants of TDP-43 nucleic acid binding domains are resistant to aggregation and have increased stability and half-life. Proc. Natl. Acad. Sci. USA *111*, 4309–4314.

32. Barmada, S.J., Skibinski, G., Korb, E., Rao, E.J., Wu, J.Y., and Finkbeiner, S. (2010). Cytoplasmic mislocalization of TDP-43 is toxic to neurons and enhanced by a mutation associated with familial amyotrophic lateral sclerosis. J. Neurosci. *30*, 639–649.

33. Woerner, A.C., Frottin, F., Hornburg, D., Feng, L.R., Meissner, F., Patra, M., Tatzelt, J., Mann, M., Winklhofer, K.F., Hartl, F.U., and Hipp, M.S. (2016). Cytoplasmic protein aggregates interfere with nucleocytoplasmic transport of protein and RNA. Science *351*, 173–176.

34. Jiang, Z., Wang, W., Perry, G., Zhu, X., and Wang, X. (2015). Mitochondrial dynamic abnormalities in amyotrophic lateral sclerosis. Transl. Neurodegener. *4*, 14.

35. Kroemer, G., Dallaporta, B., and Resche-Rigon, M. (1998). The mitochondrial death/life regulator in apoptosis and necrosis. Annu. Rev. Physiol. *60*, 619–642.

36. Galluzzi, L., and Kroemer, G. (2008). Necroptosis: a specialized pathway of programmed necrosis. Cell *135*, 1161–1163.

37. Choi, S.W., Gerencser, A.A., and Nicholls, D.G. (2009). Bioenergetic analysis of isolated cerebrocortical nerve terminals on a microgram scale: spare respiratory capacity and stochastic mitochondrial failure. J. Neurochem. *109*, 1179–1191.

38. Wang, W., Wang, X., Fujioka, H., Hoppel, C., Whone, A.L., Caldwell, M.A., Cullen, P.J., Liu, J., and Zhu, X. (2016). Parkinson's disease-associated mutant VPS35 causes mitochondrial dysfunction by recycling DLP1 complexes. Nat. Med. *22*, 54–63.

39. Wang, W., Zhang, F., Li, L., Tang, F., Siedlak, S.L., Fujioka, H., Liu, Y., Su, B., Pi, Y., and Wang, X. (2015). MFN2 couples glutamate excitotoxicity and mitochondrial dysfunction in motor neurons. J. Biol. Chem. *290*, 168–182.